[4.3.1]Bicyclic FKBP Ligands Inhibit *Legionella Pneumophila* Infection by *Lp*Mip-Dependent and *Lp*Mip-Independent Mechanisms**

Robin C. E. Deutscher[+],[a] M. Safa Karagöz[+],[b] Patrick L. Purder,[a] Jürgen M. Kolos,[a] Christian Meyners,[a] Wisely Oki Sugiarto,[a] Patryk Krajczy,[a] Frederike Tebbe,[c] Thomas M. Geiger,[a] Can Ünal,[b] Ute A. Hellmich,[c, f, g] Michael Steinert,*[b, e] and Felix Hausch*[a, d]

Legionella pneumophila is the causative agent of Legionnaires' disease, a serious form of pneumonia. Its macrophage infectivity potentiator (Mip), a member of a highly conserved family of FK506-binding proteins (FKBPs), plays a major role in the proliferation of the gram-negative bacterium in host organisms. In this work, we test our library of >1000 FKBP-focused ligands for inhibition of *Lp*Mip. The [4.3.1]-bicyclic sulfonamide turned out as a highly preferred scaffold and provided the most potent *Lp*Mip inhibitors known so far. Selected compounds were non-toxic to human cells, displayed antibacterial activity and block bacterial proliferation in cellular infection-assays as well as infectivity in human lung tissue explants. The results confirm [4.3.1]-bicyclic sulfonamides as anti-legionellal agents, although their anti-infective properties cannot be explained by inhibition of *Lp*Mip alone.

Introduction

FK506-binding proteins (FKBPs), named after the natural product FK506, which led to their discovery, belong to the protein class of immunophilins. Most FKBPs possess a peptidyl-prolyl *cis/trans* isomerase (PPIase) activity and are considered as a drug target for multiple diseases in humans.[1] FKBPs are highly conserved and found in all eukaryotes from mammals like humans and mice to fruit flies, rice and yeasts.[2] In addition, there are also microbial or parasitic FKBPs, called macrophage infectivity potentiators (Mips), which play an important role in the virulence of the pathogens.[3] Mips have been discovered in many pathogens, including *Legionella pneumophila*, *Chlamydia trachomatis*, *Burkholderia pseudomallei* and the parasites *Plasmodium falciparum* and *Trypanosoma cruzi*.[4,5] Mips are ranked among the nonessential virulence factors, which are the target of novel strategies to develop new anti-virulence drugs.[6]

The first Mip protein was identified in *L. pneumophila* (*Lp*Mip), which is a gram-negative bacterium that causes Legionnaires' disease, a serious and sometimes fatal form of pneumonia.[4,7,8] *Lp*Mip plays an important role in the early stage of infection as *Lp*Mip lacking bacteria are initially replicating at much lower rates in the infected human alveolar macrophages.[9] *Lp*Mip consists of two domains that are connected by a α-helix containing 12 turns. While the N-terminal domain facilitates homodimerization, the C-terminal

[a] R. C. E. Deutscher,[+] Dr. P. L. Purder, Dr. J. M. Kolos, Dr. C. Meyners, W. Oki Sugiarto, P. Krajczy, T. M. Geiger, Prof. Dr. F. Hausch
Institute for Organic Chemistry and Biochemistry
Technical University Darmstadt
Peter-Grünberg-Straße 4, 64287 Darmstadt (Germany)
E-mail: felix.hausch@tu-darmstadt.de

[b] M. Safa Karagöz,[+] Dr. C. Ünal, Prof. Dr. M. Steinert
Institut für Mikrobiologie
Technische Universität Braunschweig
Spielmannstr. 7, 38106 Braunschweig (Germany)
E-mail: m.steinert@tu-bs.de

[c] F. Tebbe, Prof. Dr. U. A. Hellmich
Institute of Organic Chemistry & Macromolecular Chemistry (IOMC)
Friedrich Schiller University Germany Humboldtstraße 10,
07743 Jena (Germany)

[d] Prof. Dr. F. Hausch
Centre for Synthetic Biology
Technical University of Darmstadt
64287 Darmstadt (Germany)

[e] Prof. Dr. M. Steinert
Helmholtz Centre for Infection Research
38106 Braunschweig (Germany)

[f] Prof. Dr. U. A. Hellmich
Center for Biomolecular Magnetic Resonance (BMRZ)
Goethe University
Max-von-Laue-Str. 9, 60438 Frankfurt/Main (Germany)

[g] Prof. Dr. U. A. Hellmich
Cluster of Excellence Balance of the Microverse
Friedrich Schiller University Jena
Jena (Germany)

[+] These authors contributed equally to this work.

[**] A previous version of this manuscript has been deposited on a preprint server (https://doi.org/10.26434/chemrxiv-2023-vfssm).

🖥 Supporting information for this article is available on the WWW under https://doi.org/10.1002/cbic.202300442.

ChemBioChem

Research Article
doi.org/10.1002/cbic.202300442

**Chemistry
Europe**

European Chemical
Societies Publishing

domain is closely related to the human FK506-binding protein 12 (FKBP12) and exhibits PPIase activity.[10] However, the PPIase activity does not seem to be necessary for the infectivity-promoting activity of *Lp*Mip as some mutants with a strongly diminished PPIase activity rescued the intracellular replication of *Lp*Mip-deficient bacteria.[11] The formation of the homodimer however seems to be more important for the initial replication of the bacteria in a cellular infection model as well as in guinea pigs.[12]

In the last few years several interaction partners and functions of *Lp*Mip were identified. *Lp*Mip contributes to the degradation of the extracellular matrix, by binding to collagen IV, a process which enables the penetration of the lung epithelial barrier. This interaction is reliant on the PPIase binding site and was inhibited by the PPIase inhibitors FK506 and rapamycin.[13] Furthermore, the Stringent starvation protein B (SspB), flagellin (FlaA) and the hypothetical protein Lpc2061 were identified as interaction partners. While the effect of SspB binding remains elusive, the binding of FlaA and Lpc2061 contributes to the formation of the single monopolar flagellum, which has a positive effect in the early phase of infection of macrophages. The PPIase domain of *Lp*Mip seems to be involved in the interaction with Lpc2061.[14]

Since *Lp*Mip is a relevant contributor to the infectivity of *L. pneumophila* and relevant virulence traits rely on the C-terminal PPIase domain, the PPIase domain of the protein is considered a suitable target for the development of anti-infectives for *L. pneumophila*. This approach might also be useful for other Mip containing bacteria and parasites.[6,15,16]

Due to the homology of FKBPs and Mips, FKBP inhibitors targeting the PPIase domain, like FK506, do also inhibit *Lp*Mip. To date there have been multiple attempts to find potent and selective *Lp*Mip inhibitors, with limited success.[3,16–18] The only inhibitor with a potential selectivity for *Lp*Mip over FKBPs might be peptide P290, as it was derived from the collagen IV structure binding to *Lp*Mip.[17] FK506 remains among the most potent inhibitors for *Lp*Mip. Therefore, more potent *Lp*Mip inhibitors that do not possess the immunosuppressive effects of FK506[18,19] are needed to validate *Lp*Mip inhibition as an anti-virulence concept.[20] In 2018, Pomplun and coworkers analyzed the binding properties of [4.3.1]-bicyclic sulfonamides – known FKBP inhibitors – to several human FKBPs and Mips, including *Lp*Mip.[21] They concluded that the investigated FKBP-inhibitors do inhibit Mips, similar to FK506. In an infection assay with *L. pneumophila* they observed a dose dependent inhibition of the replication of the bacteria in human THP-1 macrophages with [4.3.1]-bicyclic sulfonamide FKBP inhibitors.[21] Furthermore, our structural data recently confirmed the conserved binding mode between *Lp*Mip and human FKBPs for [4.3.1]-bicyclic sulfonamides.[22]

Building on this discovery, we screened our whole library consisting of over 1000 FKBP-focused compounds, featuring five major scaffolds for affinity towards *Lp*Mip, including the before mentioned [4.3.1]-bicyclic sulfonamide scaffold to determine the favored scaffold. We further investigated selected compounds in a set of biochemical and infection assays to refine our understanding of the mechanisms underlying the anti-virulence effects.

Results and Discussion

Screening of a FKBP-focused substance library for LpMip inhibition

First, we set out to screen our in-house library of FKBP ligands for affinity towards *Lp*Mip. This library consisted of >1000 compounds with an affinity of lower than 500 nM for FKBP12 and a molecular weight range of 400–800 Da. Some compounds of the library are published,[21,23–35] while most compounds remain unpublished. The majority of compounds can be assigned to one of five major scaffolds (Figure 1), with 33% of the compounds belonging to the class of [4.3.1]-bicyclic sulfonamides.

For the evaluation of the compounds, a fluorescence polarization (FP)-assay with a *Lp*Mip construct (77–214) missing the dimerization domain and parts of the long alpha helix was used. Gratifyingly, the tracer [16 g] from Pomplun et al. could be used for FP assays,[21] enabling a medium throughput screening in a 384-well format.

For each compound, the percentage of inhibition was determined at a concentration of 10 μM, with a cutoff for positive hits set at an inhibition of 55%. This resulted in 154 hits selected for further investigation. Of these 154 compounds, only three (rapamycin, FK506 and FK1706) were not a [4.3.1]-bicyclic sulfonamide, indicating a strong preference of *Lp*Mip for this FKBP-inhibitor scaffold.
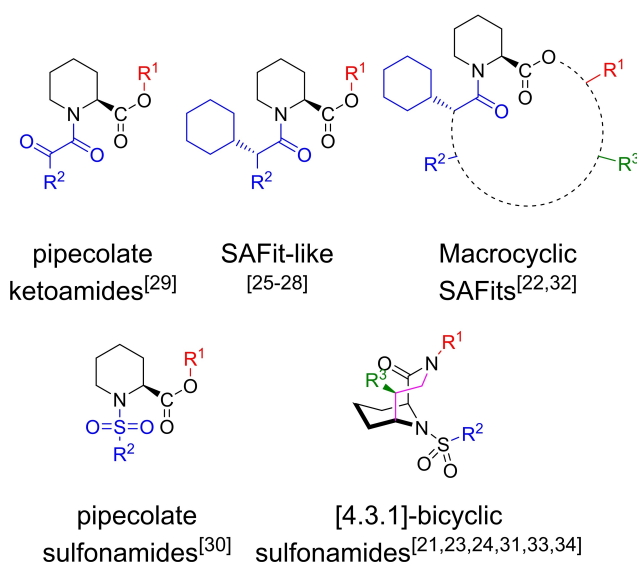

Figure 1. Primary scaffolds of the FKBP-focused compound library. The pipecolate core (black) is common to all scaffolds as well as FK506 and rapamycin. The red substituents are bound to the acid or amide part, the blue R²-group substituents are bound to the pipecolate amine, the green substituents are found at other positions on the respective scaffold and magenta represents the bridge in the [4.3.1]-bicyclic sulfonamides.[21,23–35]

ChemBioChem

Research Article
doi.org/10.1002/cbic.202300442

**Chemistry
Europe**
European Chemical
Societies Publishing

For the 154 selected compounds, dose response curves were measured to obtain the K_i-values for the inhibition of *Lp*Mip.[36] Building on the results of the dose response curves, eight FKBP inhibitors (**1**, **2**, **3**, **4a/b**, **5**, **6**, and **7a**) as well as FK506 and rapamycin were selected for further testing (Figure 2, Table 1). Compounds **5** and **6** were chosen, because they had the lowest K_i towards *Lp*Mip. Compounds **1**-**4b** were chosen to elucidate whether the clear SAR in positions R^1 and R^3 of the [4.3.1]-bicyclic sulfonamides in vitro can be translated to cellular assays. Compound **7a** was chosen due to its different R^1-group. In addition, compounds **15** and **23** were included in the further analysis as inactive and cell-impermeable controls, respectively (Scheme 1, Table 1). Furthermore, based on the results of the initial cellular assays, eight additional compounds (**7b/c/f/g**, **16**, **18a/b**, **19**; Scheme 1, Table 1) were synthesized. As compounds **1** and **7a** only differ in the R^1-position, compounds **7b/c/f/g**, **16** and **18a/b** were synthesized to extend the structure-activity relationship in that position. Compound **19**, with the R^1-substituent of **7a**, was synthesized to analyze whether the

structure-activity-relationship in the R^3-position is influenced by the differing R^1-substituent. The R^2-position was not varied as the initial screening suggested that the 3,5-dichorophenyl group is the best choice regarding affinity. All 18 compounds were tested for their affinity towards full length (1-214) as well as shortened (77-214) *Lp*Mip, to human FKBP12, for their intracellular affinity for human FKBP12 in mammalian cells[37] (Table 1), and their MIC for *L. pneumophila* (Table 2).

Additionally, all compounds were tested for cytotoxicity (Figure 3) and in cellular infection assays using A549 lung epithelial cells and THP-1 macro-phages (Table 2). For the initial 10 compounds and control compounds **15** and **23**, cellular infection assays using a *Lp*Mip-deficient variant of *L. pneumophila* were also performed (*Δmip*, Table 2). A refined subset of compounds was tested in infection assays with human lung tissue explant (figure 5E).

Synthesis of selected FKBP and LpMip inhibitors

Of the eight initial [4.3.1]-bicyclic sulfonamides chosen for further testing seven were already published and were synthesized following the published procedure (Figure 2).[21,32]

The key intermediate **13** had been synthesized before[21] but the need for higher amounts required an alternative approach. Therefore, starting from the known precursor **8**[21,32] deprotection by hydrazinolysis and reaction by reductive amination with 2-(benzyloxy)acetaldehyde provided **9**. The five subsequent steps follow the synthesis as described for compound **1**[21] yielding the protected alcohol **12**. The alcohol was then deprotected using BCl_3SMe_2 and oxidized by Jones oxidation to form carboxylic acid **13**.

The synthesis for the closely related compounds **15** and **16** followed a different route as the α-methyl group in R^1 is more
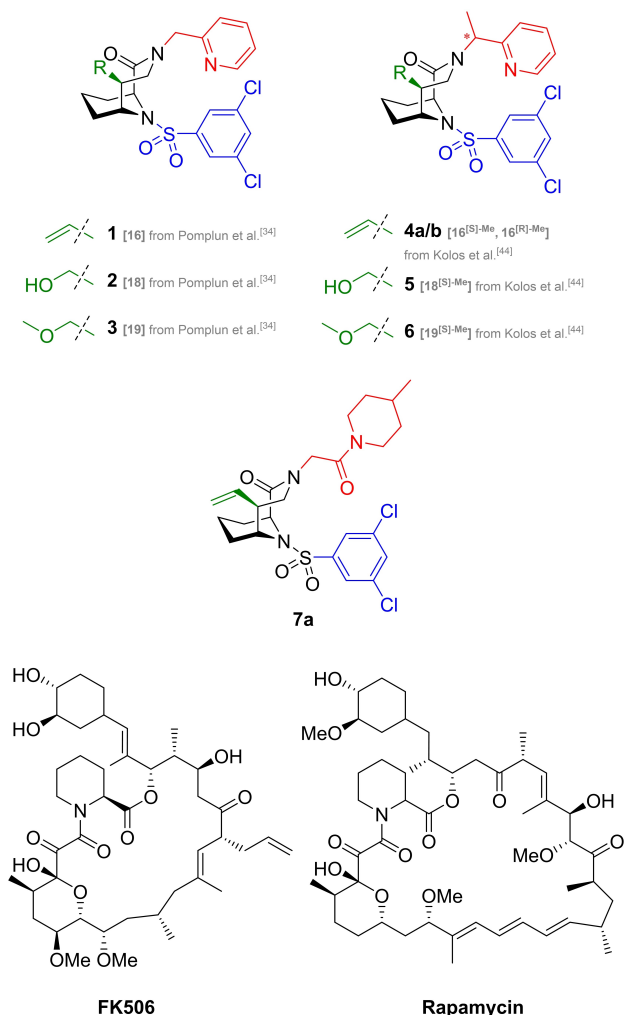

Figure 2. *Lp*Mip inhibitors selected for further characterization. Compounds **1**–**3** from Pomplun et al.34, Compounds **4a**-**6** from Kolos et al.44, compound **7a** and natural products FK506 and rapamycin. The different colors of the residues correspond to the colors chosen for the residues in scaffold in Figure 1.
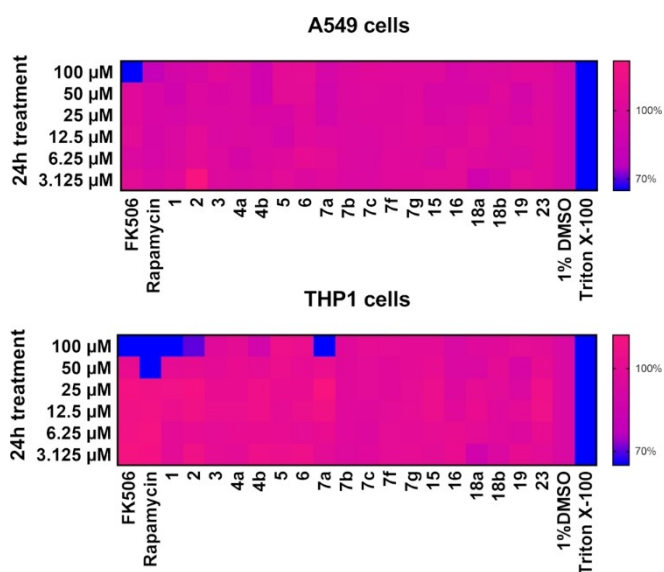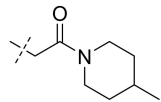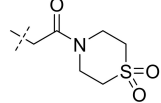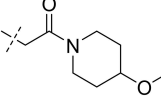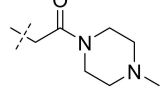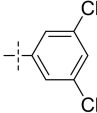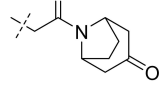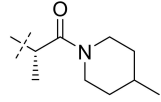

Figure 3. Cytotoxicity of substances on A549 and THP-1 cells. Triton X-100 was used as positive (toxic) control. 1 % DMSO was used as negative control. Conditions with > 70 % functional cells are counted as non-toxic.[38]

Table 1. Affinity data for binding to purified LpMip (1–214 and 77–214) and human FKBP12, determined by a fluorescence polarization assay (FP), and nanoBRET data for intracellular FKBP12 occupancy.

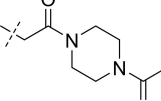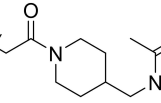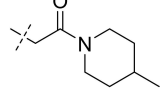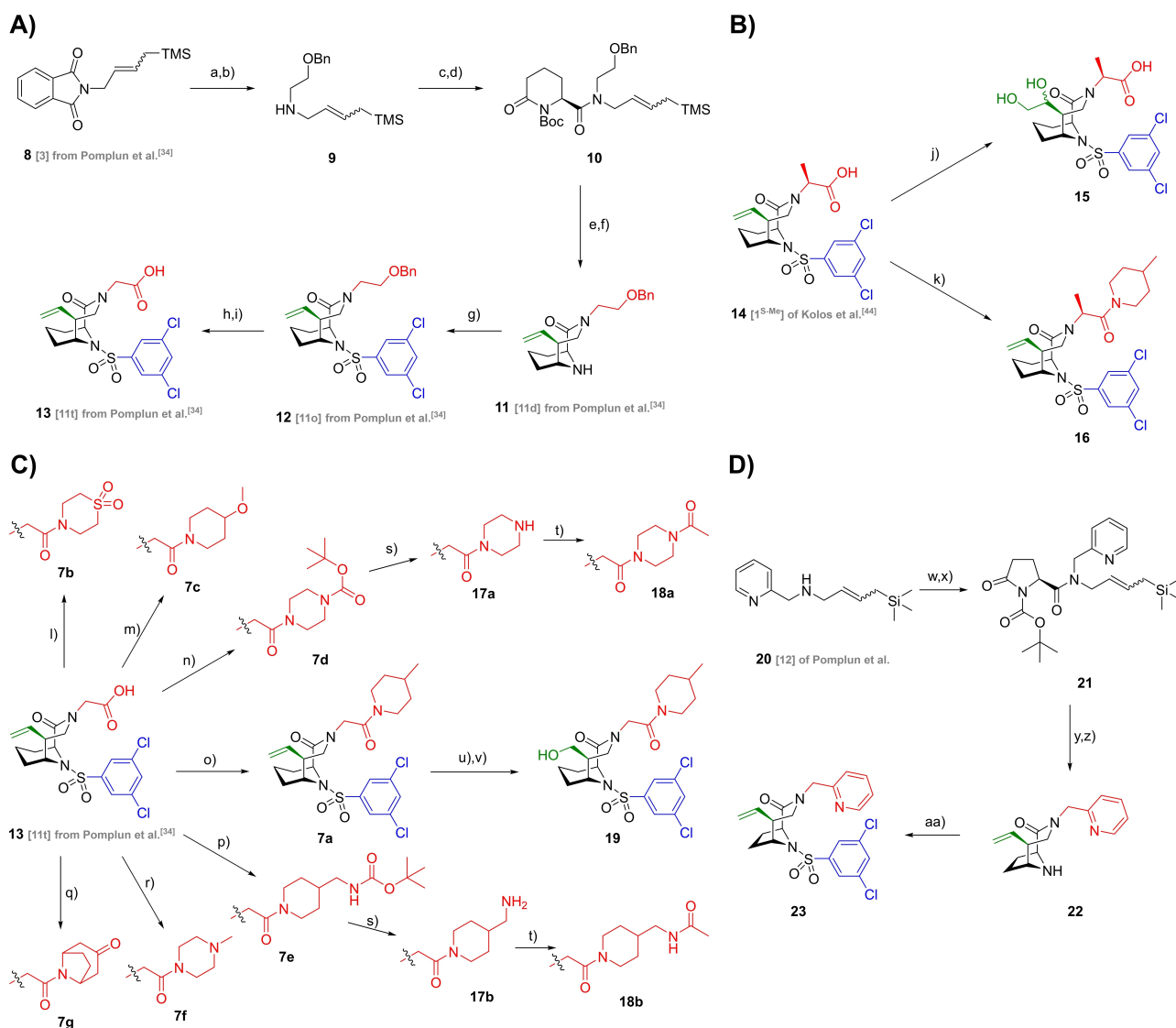| No.	LpMip (1-214) FP, K_i [nM]	LpMip (77-214) FP, K_i [nM]	human FKBP12 FP, K_i [nM]	FKBP12 nanoBRET, IC50 [nM]	R¹	R²	R³
FK506	184	144	0.2	4.7 ± 0.3	–	–	–
Rapamycin	91	347	0.6	30.3 ± 1.5	–	–	–
1	3860	3019	1.3	20.7 ± 1.7	CH₂Py		vinyl
2	97	101	0.52	5.4 ± 0.5	CH₂Py		CH₂—OH
3	419	353	0.65	5.6 ± 0.5	CH₂Py		CH₂—OMe
4a	56	47	0.72	5.4 ± 0.4	CH((S)–CH₃)Py		vinyl
4b	5320	7350	130	5788 ± 794	CH((R)–CH₃)Py		vinyl
5	7.1	6.7	0.29	7.4 ± 0.4	CH((S)–CH₃)Py		CH₂—OH
6	7.6	7.1	0.33	15.7 ± 1.3	CH((S)–CH₃)Py		CH₂—OMe
7a	708	700	0.3	3.1 ± 0.2			vinyl
7b	264	270	3.0	9.6 ± 1.0			vinyl
7c	575	627	0.66	3.1 ± 0.3			vinyl
7f	158	270	0.20	3.9 ± 0.3			vinyl
7g	2255	4070	0.65	2.4 ± 0.2			vinyl
15	22.6	19.6	1.7	5898 ± 1698	CH((S)–CH₃)COOH		CHOH—CH₂OH
16	232	248	0.26	12.1 ± 1.2			vinyl
18a	541	537	0.27	17.6 ± 1.6			vinyl
18b	244	291	0.20	5.3 ± 0.4			vinyl
19	24	41	0.022	1.2 ± 0.1			CH₂—OH
23	>10000	>10000	**1000**	4571 ± 402	CH₂Py		vinyl

conveniently installed before the formation of the [4.3.1]-bicyclic sulfonamide scaffold. Therefore, starting from compound **14** ([1S-Me] of Kolos et al.[32]), dihydroxylation was performed using osmium tetroxide, to gain compound **15** as a diastereomeric mixture. Compound **16** was obtained using an amide coupling.

ChemBioChem

Research Article
doi.org/10.1002/cbic.202300442

**Chemistry
Europe**
European Chemical
Societies Publishing

Scheme 1. Synthesis of [4.3.1]-bicyclic sulfonamides as FKBP and *Lp*Mip inhibitors (A) Large scale synthesis of key intermediate **13**. (B) Synthesis of compounds **15** and **16**, starting from **14** [1^S-Me] of Kolos et al.[32] (C) Variation of the R[1] and R[3]-groups, starting from **13**. (D) Synthesis of the inactive reference compound **23**. **Reactions and conditions:** a) hydrazine, MeOH, reflux, 16 h; b) 2-(benzyloxy)acetaldehyde, NaBH4, EtOH, rt, 4 h, 66% (two steps); c) (S)-6-oxopiperidine-2-carboxylic acid, HATU, DIPEA, DMF, rt, 2 h; d) Boc2O, DIPEA, DMAP, DCM, rt, 15 h, 74% (2 steps); e) DIBAL−H, THF, −78 °C, 3.5 h; f) HF-pyridine, −78 °C-0 °C, 1 h, 27% (2 steps); g) 3,5-dichlorobenzenesulfonyl chloride, DIPEA, MeCN, 3 d, rt, 74%; h) BCl3SMe2, DCM, rt, 2 h, 87%; i) Jones reagent, acetone, 0 °C, 2 h, 78%; j) 2,6-Lutidine, NMO, osmium tetroxide, acetone/water (9:1), rt, 25 h, 59%; k) 4-methylpiperidine, HATU, DIPEA, DMF, rt, 3 d, 42%; l) Thiomorpholine 1,1-dioxide, HBTU, HOBt, DIPEA, DMF, rt, 20 h, 91%; m) 4-methoxypiperidine hydrochloride, HBTU, HOBt, DIPEA, DMF, rt, 3 d, 98%; n) 1-piperazinecarboxylic acid, DIPEA, DMF, rt, 1 h, 92%; o) 4-methylpiperidine, HBTU, HOBt, DIPEA, DMF, rt, 3 d, 50%; p) tert-butyl-4-piperidinylmethylcarbamate, HATU, DIPEA, DMF, rt, 18 h, 70%; q) 1-methylpiperazine, HATU, DIPEA, DMF, rt, 10 d, 73%; r) nortropinone hydrochloride, HBTU, HOBt, DIPEA, DMF, rt, 18 h, 73%; s) TFA, DCM, rt, 28 h, 95% **17a**; 54% **17b**; t) acetyl chloride, DIPEA, DCM, rt, 2 h, 31% **18a**; 90% **18b**; u) osmium tetroxide, sodium periodate, 1,6-lutidine, dioxane/water (3:1), rt, 24 h; v) NaBH4, THF, rt, 1 h, 76% (2steps); w) pyroglutamic acid, EDC, HOBt, DMF, 0 °C-rt, 17 h; x) Boc2O, DIPEA, DMAP, DCM, rt, 15 h, 57% (2 steps); y) DIBAL−H, THF, −98 °C, 5 min; z) HF-pyridine, −84 °C–0 °C, 3 h, 40% (2 steps); aa) 3,5-dichlorobenzesulfonyl chloride, DIPEA, MeCN, 18 h, rt, 80%.

The carboxylic acid **13** was coupled to seven different piperidines and piperazines to form compounds **7a-g**. For compounds **7d** and **7e**, Boc deprotection with TFA followed by an acetylation with acetyl chloride was performed, yielding **18a** and **18b**. Compound **7a** was subjected to oxidative cleavage of the double bond and additional reduction of the formed aldehyde to provide alcohol **19**.

Compound **23** was originally synthesized to explore a ring contraction of the [4.3.1] ring system. This was found to dramatically compromise binding to FKBPs and *Lp*Mip. Due to

the close structural similarity, compound **23** was included in the follow-up assays as a negative control. The synthesis of compound **23** proceeded analogously to the route for [4.3.1]-bicyclic sulfonamides,[21,32] but instead of (*S*)-6-oxopiperidine-2-carboxylic acid, pyroglutamic acid was used to install the five-membered ring of the scaffold. The amide was subsequently protected with a Boc-group to obtain the precursor **21** for the key steps of chemoselective reduction and asymmetric N-acyliminium cyclisation. The DIBAL−H reduction and HF-cyclisation provided compound **22** with a yield of 40% over two steps,

ChemBioChem

Research Article
doi.org/10.1002/cbic.202300442

Chemistry Europe
European Chemical
Societies Publishing

Table 2. FP-Assay data for *Lp*Mip, bacterial MIC data for *L. pneumophila* wt and *Δmip*, cellular toxicity data for A549 lung epithelial cells and THP1 macrophages and cellular infection assays with A549 lung epithelial cells and THP1 macrophages infected with *L. pneumophila* wt and *Δmip* for all compounds.

No.	*Lp*Mip (1-214) FP / nM	Bacterial MIC		Cellular infection assay							
		wild type 24 h	*Δmip* 24 h	A549-cells wild type 24 h	A549-cells wild type 48 h	THP-1 cells wild type 24 h	THP-1 cells wild type 48 h	A549-cells *Δmip* 24 h	A549-cells *Δmip* 48 h	THP-1 cells *Δmip* 24 h	THP-1 cells *Δmip* 48 h
FK506	184										
Rapa-mycin	91										
1	3860										
2	97										
3	419										
4a	56										
4b	5320										
5	7.1										
6	7.6										
7a	708										
7b	264	n.d.						n.d.	n.d.	n.d.	n.d.
7c	575	n.d.						n.d.	n.d.	n.d.	n.d.
7f	158	n.d.						n.d.	n.d.	n.d.	n.d.
7g	2255	n.d.						n.d.	n.d.	n.d.	n.d.
15	23										
16	232	n.d.						n.d.	n.d.	n.d.	n.d.
18a	541	n.d.						n.d.	n.d.	n.d.	n.d.
18b	244	n.d.						n.d.	n.d.	n.d.	n.d.
19	24	n.d.						n.d.	n.d.	n.d.	n.d.
23	>10000										

| Effect at | >100 μM | 100 μM | 50 μM | 25 μM | 12,5 μM | 6,25 μM | 3,13 μM | Not determined |

which is similar to the cyclisation previously performed for (*S*)-6-oxopiperidine-2-carboxylic acid-based precursors.[21,32] Subsequently the R²-residue was installed using a commercially available sulfonylchloride, yielding compound **23**.

Structure-activity-relationship analysis of selected FKBP and LpMip inhibitors for LpMip

The affinities for binding to purified human FKBP12 and two constructs of *Lp*Mip were determined by a competitive FP-assay (Table 1).[21,37] The K_i-values for full length *Lp*Mip and the shortened version of *Lp*Mip were comparable in all cases (< 3-fold difference). Therefore, the structure-activity-relationship is discussed only for full-length *Lp*Mip.

The analysis revealed that for the R¹-group the introduction of a (*S*)-methyl group in the α-position of the pyridine does increase the binding affinity for *Lp*Mip by a factor of 14 to 69 for the three pairs of ligands (K_i^{LpMip} **1** = 3860 nM→**4a** = 56 nM, factor, 69; **2** = 97 nM→**5** = 7.1 nM, factor 14; **3** = 419 nM→**6** = 7.6 nM, factor 55). Conversely, the (*R*)-methyl group leads to a decrease, with the binding affinity of compound **4b** being

worse by a factor of 1.4. A similar effect has been observed for human FKBPs, which was attributed to the displacement of a conserved but energetically unfavorable water molecule.[32]

The 4-methylpiperidine in the R¹ position of **7a** is favored over the pyridine in the R¹-position by a factor of 5 (K_i^{LpMip} **1** = 3860 nM→**7a** = 708 nM) for *Lp*Mip and 4.3 (K_i^{FKBP12} **1** = 1.3 nM→**7a** = 0.3 nM) for FKBP12. Other R¹-group amide substituents led mostly to an increase in binding affinity in comparison to amide **7a** up to a factor of 4.5 for amide **7f** (K_i^{LpMip} **7a** = 708 nM→**7f** = 158 nM). Only with amide **7g** a decrease by a factor of 3 was observed, likely caused by a different conformation of the piperidine ring induced by the two carbon bridge and the ketone (K_i^{LpMip} **7a** = 708 nM→**7g** = 2255 nM). For the amide **16** an increase of binding affinity by the (*S*)-methyl group in the α-position was also observed in comparison to compound **7a**, although the increase with a factor of 3 is not as strong as with the pyridine group.

In the R³-position, the methoxymethyl group (K_i^{LpMip} **1** = 3860 nM→**3** = 419 nM, factor 9; **4a** = 56 nM→**6** = 7.6 nM, factor 7) and even more so the hydroxymethyl group (K_i^{LpMip} **1** = 3860 nM→**2** = 97 nM, factor 40; **4a** = 56 nM→**5** = 7.1 nM, factor 8) were preferred over the vinyl group.

ChemBioChem

Research Article
doi.org/10.1002/cbic.202300442

Chemistry
Europe
European Chemical
Societies Publishing

Regarding the interaction between the residues R[1] and R[3], it can be concluded that the affinity enhancing effects of the substituents in R[1]- and R[3]-position mostly do seem to be working independent to each other.

The ring contraction in [4.2.1]-bicyclic sulfonamide **23** dramatically affected binding to *Lp*Mip as well as to FKBP12, leading to >500-fold weaker binding compared to the direct [4.3.1]-bicyclic analog **1**.

Characterization of cytotoxicity and cell permeability of the inhibitors

To gain further insight into the cellular effects of the inhibitors, we investigated their cytotoxicity and cell permeability. Cytotoxicity testing was performed with A549 lung epithelial cells and THP-1 macrophages, which represent relevant cell types for *L. pneumophila* infections (Figure 3).

While some FKBP inhibitors (**1**, **7a**, FK506, rapamycin) were toxic at 100 μM in THP1 cells, none of the synthetic inhibitors were toxic at 50 μM and none were toxic to A549 cells.

To get insight into the ability of Mip/FKBP inhibitors to occupy FKBPs inside cells, a nanoBRET-assay was performed, using engineered HEK293T cells expressing a FKBP12-luc fusion construct (Table 1).[36] In general, all compounds (with the exception of **4b**, **15** and **23**) were potently able to occupy FKBP12 in human cells. In the case of **15**, the high polarity is likely responsible for a poor cell permeability.

In conclusion, our LpMip inhibitors display very low cytotoxicity and are able to penetrate cells, suggesting their suitability for functional cellular experiments.

Inhibition of growth and intracellular replication of L. pneumophila

To investigate the direct anti-legionellal activity of our *Lp*Mip/ FKBP inhibitors, it is necessary to determine their direct antibacterial properties, as the presence of pathogens is essential for the development and progression of infections. Therefore, we subjected both wild type and *Lp*Mip-deficient[8] *L. pneumophila* strains to treatment with the inhibitors to determine their minimal inhibitory concentration (MIC) (see Table 2 and Figure 4 for FK506 and **7a** as representative examples and supplement Figure S1 for all other compounds).

Except for **2**, **4b**, **15** and **23** all tested *Lp*Mip inhibitors inhibited bacterial growth at less than 100 μM. Most compounds (**1**, **4a**, **7a/b/d/g**, **18a**/b, **19**) were comparable to FK506, while **16** was slightly more potent. Overall, however, there was a poor correlation between *Lp*Mip affinity and antibacterial MIC.

Most importantly, the activities of all compounds were almost identical in wild type and *Lp*Mip-deficient *L. pneumophila* strains, clearly excluding *Lp*Mip as the relevant target in this assay. Taken together, these results show that our *Lp*Mip/ FKBP-inhibitors can inhibit the growth of *L. pneumophila* bacteria, but in an *Lp*Mip-independent manner.
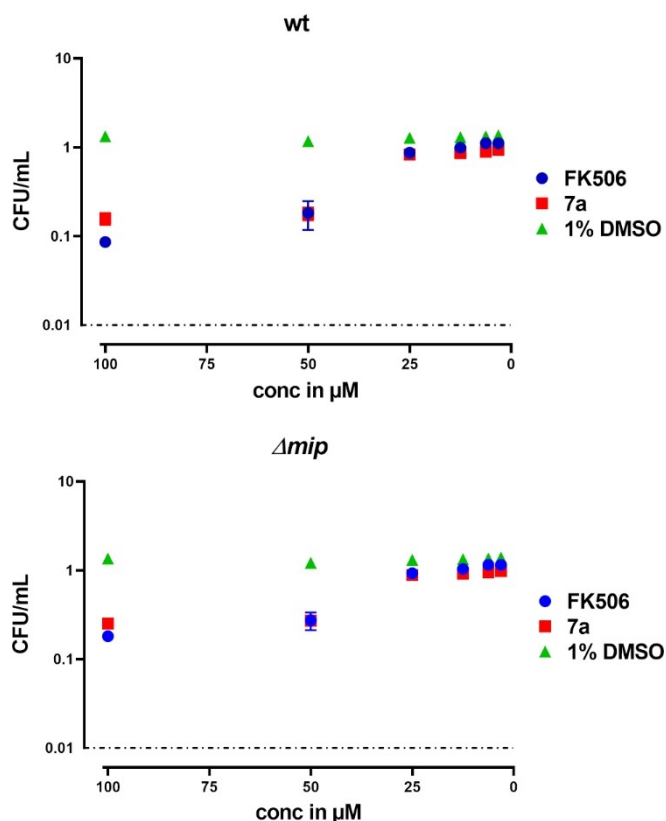

Figure 4. Impact of FK506 and compound **7a** on the growth of *L. pneumophila* wild type and *Δmip* strain after 24 hours. The bacterial growth was quantified by measuring the OD600 nm. 1% DMSO references (green triangles) were included as negative controls for each set of compound concentrations. The MIC values were determined using GraphPad regression analysis. The 95% confidence interval for the calculated values was ±5%.

To investigate the *Lp*Mip/FKBP inhibitors in a bacterial/ mammalian cellular infection assay, we treated A549 lung epithelial cells and THP-1 macrophages with *L. pneumophila* bacteria for 2 h, followed by addition of *Lp*Mip/FKBP inhibitors and counting the number of bacteria at 2 h, 24 h and 48 h (Table 2 and Figure 5 for FK506 and **7a** as representative examples). Most *Lp*Mip inhibitors with a pyridine group in R[1], except **3**, **4b**, **15**, and **23**, showed inhibition of intracellular replication of the bacteria at 25 μM after 24 h and 48 h in both cell types (supplement Figures S2, S3). The inactivity of **15** can be explained by lack of cell permeability, while the lack of activity of compounds **4b** and **23** is in line with generally poor *Lp*Mip/FKBP inhibition. Remarkably, compound **7a** inhibited intracellular replication at a concentration of 6.25 μM in both cell types after 24 h and 48 h (Figure 5A and 5B). However, even small changes, like exchanging the methylpiperidine **7a** with the methylpiperazine **7f** or a methoxypiperidine **7c** or adding a methyl group (compound **16**) dramatically increase the minimal concentration for inhibition of intracellular replication. While compound **19** with a change in the R[3]-position still retains some inhibitory effect, larger changes in the R[1]-position like for compounds **7g**, **18a** and **18b** eliminate almost any inhibitory effect.
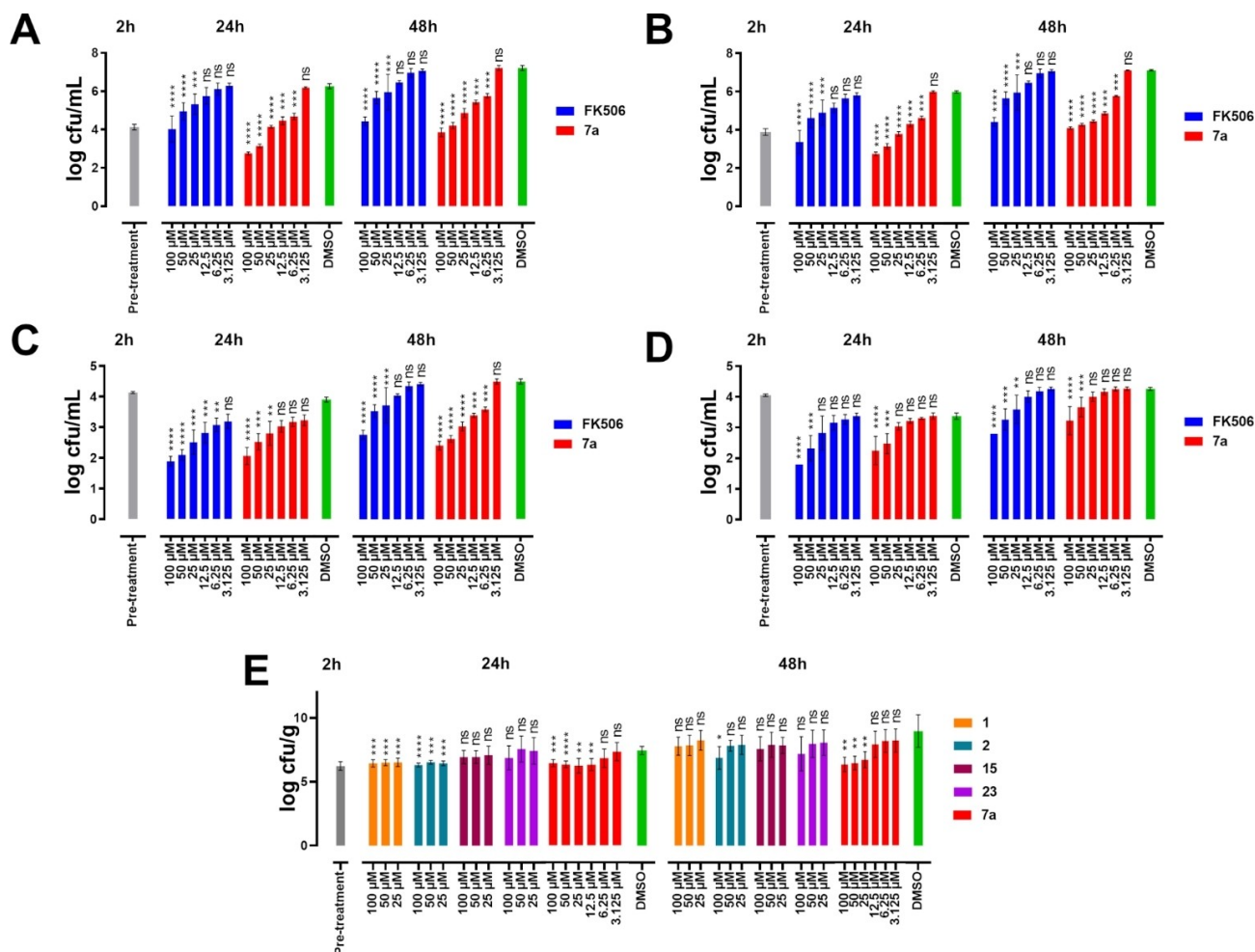
Figure 5. Intracellular replication of *L. pneumophila* wild type (wt, A and B) and *Δmip* strains (C and D) in A549 lung epithelial cells (A and C) and THP1 macrophages (B and D) was determined following 24 and 48 hours of exposure to different substance concentrations. Additionally, intracellular replication of *L. pneumophila* wild type strains in human lung tissue explants (HLTEs) was analyzed after 24 and 48 hours of exposure to various substance concentrations (E). The results obtained at 24 and 48 hours are presented and compared to the control group, which consisted of 1% DMSO. A Dunnet's multiple comparison test was performed on 12 replicates, respective 6 replicates for the cellular infection assays with the *L. pneumophila* wild type (wt, A and B) and the *Δmip* strains. 7 replicates were used for the HLTE. Statistical significance is indicated by * for $p < 0.05$, ** for $p < 0.01$, *** for $p < 0.001$, **** for $p < 0.0001$, and ns for not significant.

Compound **7b** containing a cyclic sulfone is the best of the R^1 analogs of **7a**, possibly by mimicking the spatial and electronic properties of the methyl group. Importantly, there was a clear disconnect between *Lp*Mip inhibition and intracellular MIC in mammalian cells, arguing against *Lp*Mip as the relevant target.

We therefore repeated the infection assay using *Lp*Mip-deficient *L. pneumophila*. Most *Lp*Mip/FKBP inhibitors, including **7a**, still significantly inhibited intracellular *L. pneumophila* replication even in the absence of *Lp*Mip, which further challenged the role of *Lp*Mip or its FK506-binding site (Figures 5C and D and supplement figure S4).

To further investigate the effect of *Lp*Mip/FKBP inhibitors on *L. pneumophila* dissemination in a relevant tissue setting, we tested the ability of five of our compounds (**1**, **2**, **7a**, **15** and **23**) to inhibit the growth of *L. pneumophila* in human lung tissue explants (HLTE). For this assay, the HLTE that were freshly prepared from human biopsies were treated with *L. pneumo-*

phila for two hours, followed by incubation for 24 h and 48 h in the presence of inhibitors (Figure 5E). Due to the limited availability of the tissue, only 3 concentrations were measured for compounds **1**, **2**, **15** and **23** in accordance with the minimal concentration of activity in the cellular infection assay.

Compounds **15** and **23** did not significantly inhibit intracellular replication compared to the DMSO control. This is consistent with their *Lp*Mip/FKBP inhibition and cellular permeability profile. For compounds **1** and **2** a significant inhibition of the replication of the bacteria is observed at a concentration of 25 μM after 24 h (Figure 5E), similar to FK506 (supplement Figure S5). Only compound **2** exhibited residual inhibitory activity at 100 μM after 48 h. Most notably, compound **7a** stands out, inhibiting intracellular replication at 12.5 μM after 24 h and at 25 μM after 48 h, making **7a** the only compound to significantly suppress the intracellular replication at 48 h. This again does not correlate with the binding affinities for *Lp*Mip.

ChemBioChem

Research Article
doi.org/10.1002/cbic.202300442

**Chemistry
Europe**
European Chemical
Societies Publishing

Conclusions

Taken together, we identified [4.3.1]-bicyclic sulfonamides as a privileged class for *Lp*Mip inhibitors, incl. compound **5** as the so far highest affinity ligand for *Lp*Mip. This is in line with trends observed for human FKBPs, where [4.3.1]-bicyclic sulfonamides routinely outperformed all other classes of FKBP ligands.[21,32] We further provide clear evidence that [4.3.1]-bicyclic Mip/FKBP ligands can reduce intracellular replication of *L. pneumophila* in pure bacterial cultures, in mammalian co-culture settings as well as in HLTE, suggesting Mip/FKBP inhibitors as potential anti-legionellal agents. However, we also observed a clear disconnect between the anti-legionellal effects and *Lp*Mip inhibition, which together with persisting effects on *Lp*Mip-deficient *L. pneumophila* strains clearly devalidate *Lp*Mip as the sole target for our inhibitors. Nevertheless, we cannot exclude *Lp*Mip is responsible for a part of the observed effect, as compounds **4a** and **7a** do inhibit wildtype *Legionella* better than *Lp*Mip-deficient *Legionella*. Based on these findings, we propose that while the FK506 binding site of LpMip is not crucial for intracellular replication of L. pneumophila, its FK506 binding site-independent function plays an important role.

Our SAR data and the control compounds employed allow to define the profile of the putative target of our compounds, which we hypothesize to be an intracellular FKBP-like protein. This is based on the following observations: (i) the inactivity of compound **23** compared to close FKBP pan-selective analogs such as **1** or **2** strongly point to an FKBP-like protein; (ii) the highly reduced activity of **4b** compared to its diastereomer **4a** is signature of all FKBPs studied so far;[31] (iii) the inactivity of cell-impermeable **15** points towards an intracellular target; (iv) the tight SAR around the methylpiperidine in the R¹ position of **7a** argues against well characterized FKBPs such as human FKBP12, FKBP51 and FKBP52. The putative FKBP-like target may be from *L. pneumophila*, which harbors trigger factor as the closest FKBP12/*Lp*Mip-like protein. Alternatively, one of the less well characterized 17 human FKBPs may serve as a host factor for *L. pneumophila*.[39] Therefore, it appears promising to identify further Mip-independent binding partners by interactomic approaches. The identified binding partners could then be subjected to a screening with our FKBP-focused ligand library. Alternatively, a direct screening in functional assays might be warranted.

Taken together, **7a** represents a promising starting point for the development of anti-legionellal agents. The identification of its target will be crucial to further optimize this compound class as anti-legionellal agents, which could also open an opportunity for other pathogens.

Experimental Section

Compound synthesis and characterization

If not indicated otherwise, reagents and solvents were purchased from commercial suppliers and used without further treatment. All reactions were followed by TLC analysis or LCMS. Flash silica gel column chromatography was performed with a Biotage® Isolera

One system with Biotage® Sfär Silica HC D columns. Column chromatography was performed manually with silica gel 60 (0.04–0.063 mm) from Machery Nagel GmbH & Co. KG. Semi-Preparative HPLC was performed with an Interchim PuriFlash 5250 system with a Luna® 5 μm C18(2) 100 Å, 250x21.2 mm column from Phenomenex. Eluents were 0.1% TFA in water (Eluent A) and 0.1% TFA in acetonitrile (Eluent B), methods are given in percentage B. All key compounds were >95% purity by HPLC. Compound purity and low-resolution mass spectra were determined using an Agilent 1260 Infinity II system with a Poroshell 120 EC–C18 1.9 μm, 2.1×50 mm column from Agilent. Eluents were 0.1% formic acid in water (Eluent A) and 0.1% formic acid in acetonitrile (Eluent B), the used method was 5% B to 100% B in 2 min. MS was recorded with an Agilent InfinityLab G6125B LC/MSD. NMR spectroscopy was performed by the NMR department at TU Darmstadt. NMR spectra were recorded either on a 300 MHz Avance II NMR spectrometer from Bruker BioSpin GmbH (for 1H-NMR only), a 300 MHz Avance III NMR spectrometer from Bruker BioSpin GmbH (for ¹H-, ¹³C-NMR), or a 500 MHz NMR spectrometer DRX 500 from Bruker BioSpin GmbH (for ¹H- and ¹³C-NMR). NMR spectra were recorded at room temperature. Chemical shifts are given in parts per million, referenced to the respective solvent (¹H: $CDCl_3 = 7.26$ ppm, $[D_6]$ DMSO $= 2.50$ ppm, ¹³C: $CDCl_3 = 77.16$ ppm, $[D_6]$ DMSO $= 39.52$ ppm). Coupling constants (J) are given in hertz (Hz), peak multiplicities are given as singlet (s), doublet (d), triplet (t), quartet (q) or multiplet (m). HRMS was performed by the mass spectrometry department at TU Darmstadt. Mass spectra were recorded on an Impact II, quadrupol-time-of-flight spectrometer from Bruker Daltonics. TLC was performed on TLC Silica gel 60 F254 Aluminum sheets from Merck Millipore. All final test compounds had a purity ≥95% as determined by HPLC and UV detection at 220 nm.

The synthesis of compounds **1–6**, **8**, **14** and **20** is described by Pomplun *et al.*[34] and Kolos *et al.*.[32] Compound **1** is **16a** of Pomplun *et al.*,[21] Compound **2** is **16h** of Pomplun *et al.*,[21] Compound **3** is **16j** of Pomplun *et al.*,[21] Compound **4a** is **16**[S]−Me of Kolos *et al.*,[32] Compound **4b** is **16**[R]−Me of Kolos *et al.*,[32] Compound **5** is **18**[S]−Me of Kolos *et al.*,[32] Compound **6** is **19**[S]−Me of Kolos *et al.*,[32] Compound **8** is **3** of Pomplun *et al.*,[21] Compound **14** is **1**[S]−Me of Kolos *et al.*[32] and Compound **20** is **12** of Pomplun *et al.*.[21]

Expression and purification of LpMIP constructs

Genes encoding N-terminally His6-tagged *Lp*MIP (1-214) or *Lp*MIP (77-214) in a pET11a vector were purchased from GenScript. Proeins were expressed in E. coli BL21 gold (DE3) cells (Agilent Technologies) grown in LB-medium supplemented with 1 mg/mL Ampicillin at 37 °C. Expression was induced at OD600 nm of 0.8 with 2 mM IPTG (final concentration). Cells were further grown at 37 °C for 4 h and harvested via centrifugation. Cell pellets were stored at −20 °C until further use. After suspension in lysis buffer (20 mM Tris pH 8, 20 mM imidazole, 300 mM NaCl, 0.1% Triton X100, 1 mM DTT, 1 mM benzamidine, 1 mM PMSF, lysozyme, DNase, RNase), cells were lyzed via sonication. The supernatant after centrifugation (45 min at 10,000 xg at 4 °C) was applied to a NiNTA gravity flow column (Qiagen). After washing with 20 mM Tris pH 8, 20 mM imidazole, 300 mM NaCl, the protein was eluted with 20 mM Tris pH 8, 500 mM imidazole, 300 mM NaCl. Imidazole was removed via dialysis over night in the presence of TEV protease in a molar ratio of 20:1 to remove the His6-tag. A reverse NiNTA gravity flow column was used to separate cleaved protein which was then further purified via size exclusion chromatography (HiLoad Superdex S200 16/60 column, GE Healthcare) with 50 mM Tris pH 7, 150 mM NaCl. Purified proteins were concentrated via VivaSpin centrifugal concentrators (Merck) and stored at −20 °C.

ChemBioChem

Research Article
doi.org/10.1002/cbic.202300442

Chemistry
Europe
European Chemical
Societies Publishing

Fluorescence Polarization assay for the determination of the binding affinity

FKBP12 was recombinantly expressed in E. coli BL21DE3Gold and had a final purity of >95% as visually judged by Coomassie gel and SEC. The proteins were stored in HEPES buffer (20 mM HEPES, 20 mM NaCl (150 mM NaCl for FKBP12.6), +/- 5% (v/v) Glycerol, pH 8.0). The fluorescent ligand was developed by Pomplun et al..[21] For most pipetting steps, a Beckman Coulter FXP Laboratory Automation Workstation was used. The compound was diluted in 1:2 serial dilutions in DMSO and then mixed in technical duplicates with protein and tracer in buffer (20 mM HEPES, pH 8.0, 0.002% v/v Triton X-100, 150 mM NaCl) in a black, non-binding 384-well plate, and then incubated with light protection for 30 min. Polarization was measured on a Tecan Spark at room temperature with an excitation wavelength of 535 nm and an emission wavelength of 595 nm.

Fluorescence Polarization assay for the medium throughput screening

For the medium throughput screening the compounds were used at a concentration of 10 μM, the protein LpMip(77-214) was used at 100 nM and the fluorescent ligand was used at a concentration of 1 nM. For each compound the percentage of inhibition was measured four times. The percentage of inhibition was determined by normalizing the polarisation of the DMSO control, without any compound to 1.00 and the polarisation of the Rapamycin control (10 μM Rapamycin) to 0.00. Each compound that exhibited a polarisation of ≤0.45, therefore had a percentage of inhibition of ≥55%.

nanoBRET-Assay for FKBP12

A FKBP ligand dilution series was performed at a 100-fold concentration of the final sample in DMSO. Next, the ligands were diluted to a 2-fold concentration required for the final sample in Opti-MEM reduced serum medium (gibco, REF 11058–021) and 20 μL were transferred to a white non-binding 384 assay plate (greiner REF 781904). HEK293T cells stably expressing FKBP12-NanoLuc[37] were detached from a cell culture dish and suspended in Opti-MEM reduced serum medium at a concentration of 9.05×10^5 cells/mL. The fluorescent tracer [2b from Gnatzy et al.[37]] was diluted to 160 nM and in Opti-MEM. Afterwards, a cell-tracer mixture was prepared by mixing 3 parts detached cells with one part of the 8-fold tracer dilution (e.g. 6.6 mL detached cells + 2.2 mL 8-fold tracer solution), yielding a 2-fold cell-tracer mix. 20 μL of the 2-fold cell tracer mix were added on top of the compound solution to the assay plate, which is briefly spun down, sealed with aluminum foil and incubated at 37 °C for 2 h. Afterwards the assay plates were equilibrated at room temperature for 15 min. For BRET detection, 20 μL of 7.5 μM extracellular Nluc-Inhibitor (compound **43**[40]) + 6.6 μM furimazine (compound **26dl**[41]) dissolved in Opti-MEM were added. The donor and acceptor emissions were measured at 445–470 nm and 610–700 nm in a well-wise measuring mode (Tecan Spark) for 1 sec, respectively. The IC_{50}-values were determined by a four-parameter fitting by GraphPad Prism version 8.0 for Windows (GraphPad Software, La Jolla, CA).

Cultivation of bacteria and MIC assays

L. pneumophila Corby wild type[42] and Δmip[11] strains were grown on Buffered Charcoal Yeast Extract (BCYE) agar (10 g/L yeast extract and 10 g/L ACES (N-(2-Acetamido)-2-aminoethanesulfonic acid) buffer [pH 6.9] supplemented with 0.4 g/L L-cysteine, 0.25 g/L iron (III) nitrate, 15 g/L agar, and 20 μg/mL kanamycin for mutant strains). Plate grown bacteria were used to inoculate Buffered Yeast Extract (YEB) medium (10 g/L yeast extract, 10 g/L ACES buffer [pH 6.9] supplemented with 0.4 g/L L-cysteine and 0.25 g/L iron (III) pyrophosphate), and the cultures were grown till they reached stationary growth phase. Bacteria were adjusted to an OD_{600nm} of 0.01 in YEB, and let grown with substances at concentrations ranging from 100 μM to 3,125 μM in a volume of 100 μL for 24 h. Bacterial growth was measured at OD_{600nm} using a microplate fluorimeter (TECAN Infinite® M Nano).

Cultivation of cell lines and cytotoxicity assays

A549 (DSMZ ACC 107) lung epithelial cells were grown in RPMI medium + 10% FCS at 37 °C and 5% CO_2. Confluent cultures were trypsinized, and adjusted to 10^5 cells/mL in fresh RPMI medium + 10% FCS. For cytotoxicity and infection assays, 100 μL of this suspension were transferred into the wells of a 96-well-plate, and the cells were grown for 24 h. Thereafter, the culture medium was replaced by 100 μL fresh medium supplemented with a substance of interest at different concentrations ranging from 100 μM to 3.125 μM. THP-1 (DSMZ ACC 16) macrophages were grown as a suspension culture in RPMI medium + 10% FCS at 37 °C and 5% CO_2. For cytotoxicity and infection assays, the cells were adjusted to 10^5 cells/mL in culture medium that was supplemented with 100 nM PMA (phorbol 12-myristate 13-acetate) in order to induce their differentiation to macrophages, and 100 μL of this suspension were transferred into the wells of a 96-well-plate. After 48 hours the differentiation medium was removed and the cells were treated with the substances as described for A549 cells.

For measuring cell viability, 20 μL resazurin solution (0.15 mg/mL resazurin sodium salt from Sigma Aldrich® Lot # MKBZ8592 V dissolved in PBS pH 7.4 and filtrated through 0.2 μm filter) was added to each well and incubated for 3 hours at 37 °C and 5% CO_2. The produced resorufin was measured with a 560 nm excitation/ 590 nm emission filter set in a microplate fluorimeter (TECAN Infinite® M Nano).

Infection assays with cell lines and human lung tissue explants (HLTEs)

L. pneumophilia strains were grown on BCYE agar. Plate grown bacteria were resuspended in RPMI medium + 10% FCS at a density of 10^6 cells/mL, and 100 μL/well were used to replace the medium of A549 cells or THP-1 cells grown for 24 h or differentiated for 48 h in 96-well-plates, respectively, resulting in a multiplicity of infection (MOI) of 1. After 2 h of incubation at 37 °C and 5% CO_2, the cells were washed three times with prewarmed PBS to eliminate the extracellular bacteria. The substances were dissolved in 100 μL RPMI + 10% FCS with concentrations ranging from 100 μM to 3.125 μM and given to the infected cells. The bacterial uptake was monitored by lysing the cells with 0.1% (v/v) Triton X-100 and plating out serial dilutions on BCYE agar plates. The intracellular replication of bacteria was monitored by repeating this procedure after 24 h and 48 h post infection.

HLTE were cut into pieces of approximately 100 mg and suspended in 1 mL RPMI medium + 10% FCS supplemented with 20 mM HEPES and 1 mM sodium pyruvate in 24-well-plates. In parallel, plate grown bacteria were adjusted to 10^7 cfu/mL in this medium, and 1 mL of this suspension was added to each well. After 2 h of incubation at 37 °C and 5% CO_2, the cells are washed three times with prewarmed PBS to eliminate the extracellular bacteria. After that, the HLTE were covered with 1 mL medium containing the substances. The substances were solved in 1 mL RPMI medium +

ChemBioChem

Research Article
doi.org/10.1002/cbic.202300442

Chemistry
Europe
European Chemical
Societies Publishing

10% FCS supplemented with 20 mM HEPES and 1 mM sodium pyruvate with a concentration ranging from 100 μM to 3.125 μM. For monitoring bacterial uptake and replication HLTE were homogenized 2, 24 and 48 h post infection, respectively, with Polytron® PT 2500 E, and serial dilutions were plated out on BCYE agar plates.

Statistical analyses

The cytotoxicity results were compared to the production of resorufin from cells treated with 1% DMSO. A compound was considered non-toxic if it resulted in at least 70% of the cells remaining alive after 24-hour treatment.[38] The percentage of living cells was measured from 7 replicates and analyzed statistically. The minimal inhibitory concentration (MIC) was also compared to that of 1% DMSO-treated bacteria. EC_{50} values were calculated from 12 replicates using GraphPad Prism version 8.2.0 for Windows (Graph-Pad Software, La Jolla, CA). The MIC was calculated according to a previously established method.[43] Infection assays were measured by comparing to 1% DMSO treated infection. A 2-way ANOVA analysis was performed on 12 replicates of cell lines infected with wild-type strains and 6 replicates infected with Δmip strains, after log transformation of the cfu/mL values. The analysis was further supplemented with a Dunnett's multiple comparison test. The IC_{50} values were also measured at 24 and 48 hours. In addition, statistical analysis was conducted on 7 replicates of HLTE infections, compared to 1% DMSO-treated HLTE infections, employing a 2-way ANOVA with a randomized block design and post-hoc testing (either Tukey's or Sidak's) for simple effect analysis, after log transformation of the cfu/g values. The analysis was further augmented with a Dunnett's multiple comparison test.

Conflict of Interests

The authors declare no competing financial interest.

Data Availability Statement

The data that support the findings of this study are available in the supplementary material of this article.

Keywords: Antiinfective · *Legionella pneumophila* · Inhibitors · Isomerases · Medicinal chemistry

[1] a) G. Balsevich, A. S. Häusl, C. W. Meyer, S. Karamihalev, X. Feng, M. L. Pöhlmann, C. Dournes, A. Uribe-Marino, S. Santarelli, C. Labermaier, K. Hafner, T. Mao, M. Breitsamer, M. Theodoropoulou, C. Namendorf, M. Uhr, M. Paez-Pereda, G. Winter, F. Hausch, A. Chen, M. H. Tschöp, T. Rein, N. C. Gassen, M. V. Schmidt, *Nat. Commun.* **2017**, *8*, 1725; b) M. W. Harding, A. Galat, D. E. Uehling, S. L. Schreiber, *Nature* **1989**, *341*, 758; c) M. Maiarù, K. K. Tochiki, M. B. Cox, L. V. Annan, C. G. Bell, X. Feng, F. Hausch, S. M. Géranton, *Sci. Transl. Med.* **2016**, *8*, 325ra19; d) L. A. Stechschulte, B. Qiu, M. Warrier, T. D. Hinds, M. Zhang, H. Gu, Y. Xu, S. S. Khuder, L. Russo, S. M. Najjar, B. Lecka-Czernik, W. Yong, E. R. Sanchez, *Endocrinology* **2016**, *157*, 3888; e) C. L. Storer, C. A. Dickey, M. D. Galigniana, T. Rein, M. B. Cox, *Trends Endocrinol. Metab.* **2011**, *22*, 481.
[2] a) J. C. Ahn, D.-W. Kim, Y. N. You, M. S. Seok, J. M. Park, H. Hwang, B.-G. Kim, S. Luan, H.-S. Park, H. S. Cho, *BMC Plant Biol.* **2010**, *10*, 253; b) G. Ghartey-Kwansah, Z. Li, R. Feng, L. Wang, X. Zhou, F. Z. Chen, M. M. Xu, O. Jones, Y. Mu, S. Chen, J. Bryant, W. B. Isaacs, J. Ma, X. Xu, *BMC Dev. Biol.* **2018**, *18*, 7.
[3] C. M. Ünal, M. Steinert, *Microbiol. Mol. Biol. Rev.* **2014**, *78*, 544.
[4] N. P. Cianciotto, B. I. Eisenstein, C. H. Mody, G. B. Toews, N. C. Engleberg, *Infect. Immun.* **1989**, *57*, 1255.
[5] a) A. G. Lundemose, S. Birkelund, S. J. Fey, P. M. Larsen, G. Christiansen, *Mol. Microbiol.* **1991**, *5*, 109; b) P. Monaghan, D. B. Leneghan, W. Shaw, A. Bell, *Parasitology* **2017**, *144*, 869; c) A. Moro, F. Ruiz-Cabello, A. Fernández-Cano, R. P. Stock, A. González, *EMBO J.* **1995**, *14*, 2483; d) I. H. Norville, N. J. Harmer, S. V. Harding, G. Fischer, K. E. Keith, K. A. Brown, M. Sarkar-Tyson, R. W. Titball, *Infect. Immun.* **2011**, *79*, 4299.
[6] C. Baron, *Curr. Opin. Microbiol.* **2010**, *13*, 100.
[7] A. A. Khweek, A. Amer, *Front. Microbiol.* **2010**, *1*, 133.
[8] J. E. McDade, C. C. Shepard, D. W. Fraser, T. R. Tsai, M. A. Redus, W. R. Dowdle, *N. Engl. J. Med.* **1977**, *297*, 1197.
[9] N. P. Cianciotto, B. S. Fields, *Proc. Natl. Acad. Sci. USA* **1992**, *89*, 5188.
[10] a) G. Fischer, H. Bang, B. Ludwig, K. Mann, J. Hacker, *Mol. Microbiol.* **1992**, *6*, 1375; b) A. Riboldi-Tunnicliffe, B. König, S. Jessen, M. S. Weiss, J. Rahfeld, J. Hacker, G. Fischer, R. Hilgenfeld, *Nat. Struct. Biol.* **2001**, *8*, 779; c) B. Schmidt, J. Rahfeld, A. Schierhorn, B. Ludwig, J. Hacker, G. Fischer, *FEBS Lett.* **1994**, *352*, 185.
[11] E. Wintermeyer, B. Ludwig, M. Steinert, B. Schmidt, G. Fischer, J. Hacker, *Infect. Immun.* **1995**, *63*, 4576.
[12] R. Köhler, J. Fanghänel, B. König, E. Lüneberg, M. Frosch, J.-U. Rahfeld, R. Hilgenfeld, G. Fischer, J. Hacker, M. Steinert, *Infect. Immun.* **2003**, *71*, 4389.
[13] a) C. M. Ünal, M. Steinert, *Biochim. Biophys. Acta* **2015**, *1850*, 2096; b) C. Wagner, A. S. Khan, T. Kamphausen, B. Schmausser, C. Unal, U. Lorenz, G. Fischer, J. Hacker, M. Steinert, *Cell. Microbiol.* **2007**, *9*, 450.
[14] M. S. Karagöz, C. M. Ünal, B. E. Mayer, M. Müsken, J. M. Borrero-de Acuña, M. Steinert, *Infect. Immun.* **2022**, *90*, e0027622.
[15] a) J. M. Kolos, A. M. Voll, M. Bauder, F. Hausch, *Front. Pharmacol.* **2018**, *9*, 1425; b) N. J. Scheuplein, N. M. Bzdyl, E. A. Kibble, T. Lohr, U. Holzgrabe, M. Sarkar-Tyson, *J. Med. Chem.* **2020**, *63*, 13355.
[16] H. O. Sintim, J. A. I. Smith, J. Wang, S. Nakayama, L. Yan, *Future Med. Chem.* **2010**, *2*, 1005.
[17] C. Ünal, K. F. Schwedhelm, A. Thiele, M. Weiwad, K. Schweimer, F. Frese, G. Fischer, J. Hacker, C. Faber, M. Steinert, *Cell. Microbiol.* **2011**, *13*, 1558.
[18] C. Christner, R. Wyrwa, S. Marsch, G. Küllertz, R. Thiericke, S. Grabley, D. Schumann, G. Fischer, *J. Med. Chem.* **1999**, *42*, 3615.
[19] a) C. Juli, M. Sippel, J. Jäger, A. Thiele, M. Weiwad, K. Schweimer, P. Rösch, M. Steinert, C. A. Sotriffer, U. Holzgrabe, *J. Med. Chem.* **2011**, *54*, 277; b) F. Seufert, M. Kuhn, M. Hein, M. Weiwad, M. Vivoli, I. H. Norville, M. Sarkar-Tyson, L. E. Marshall, K. Schweimer, H. Bruhn, P. Rösch, N. J. Harmer, C. A. Sotriffer, U. Holzgrabe, *Bioorg. Med. Chem.* **2016**, *24*, 5134.
[20] S. L. Schreiber, G. R. Crabtree, *Immunol. Today* **1992**, *13*, 136.
[21] S. Pomplun, C. Sippel, A. Hähle, D. Tay, K. Shima, A. Klages, C. M. Ünal, B. Rieß, H. T. Toh, G. Hansen, H. S. Yoon, A. Bracher, P. Preiser, J. Rupp, M. Steinert, F. Hausch, *J. Med. Chem.* **2018**, *61*, 3660.
[22] C. Wiedemann, J. J. Whittaker, V. H. Pérez Carrillo, B. Goretzki, M. Dajka, F. Tebbe, J.-M. Harder, P. Krajczy, B. Joseph, F. Hausch, A. Guskov, U. A. Hellmich, **2023**, arXiv preprint DOI: 10.1101/2023.04.24.538046.
[23] M. Bauder, C. Meyners, P. L. Purder, S. Merz, W. O. Sugiarto, A. M. Voll, T. Heymann, F. Hausch, *J. Med. Chem.* **2021**, *64*, 3320.
[24] M. Bischoff, P. Mayer, C. Meyners, F. Hausch, *Chem. Eur. J.* **2020**, *26*, 4677.
[25] M. Bischoff, C. Sippel, A. Bracher, F. Hausch, *Org. Lett.* **2014**, *16*, 5254.
[26] X. Feng, C. Sippel, A. Bracher, F. Hausch, *J. Med. Chem.* **2015**, *58*, 7796.
[27] X. Feng, C. Sippel, F. H. Knaup, A. Bracher, S. Staibano, M. F. Romano, F. Hausch, *J. Med. Chem.* **2020**, *63*, 231.
[28] S. Gaali, X. Feng, A. Hähle, C. Sippel, A. Bracher, F. Hausch, *J. Med. Chem.* **2016**, *59*, 2410.
[29] S. Gaali, A. Kirschner, S. Cuboni, J. Hartmann, C. Kozany, G. Balsevich, C. Namendorf, P. Fernandez-Vizarra, C. Sippel, A. S. Zannas, R. Draenert,

E. B. Binder, O. F. X. Almeida, G. Rühter, M. Uhr, M. V. Schmidt, C. Touma, A. Bracher, F. Hausch, *Nat. Chem. Biol.* **2015**, *11*, 33.

[30] R. Gopalakrishnan, C. Kozany, S. Gaali, C. Kress, B. Hoogeland, A. Bracher, F. Hausch, *J. Med. Chem.* **2012**, *55*, 4114.

[31] R. Gopalakrishnan, C. Kozany, Y. Wang, S. Schneider, B. Hoogeland, A. Bracher, F. Hausch, *J. Med. Chem.* **2012**, *55*, 4123.

[32] J. M. Kolos, S. Pomplun, S. Jung, B. Rieß, P. L. Purder, A. M. Voll, S. Merz, M. Gnatzy, T. M. Geiger, I. Quist-Løkken, J. Jatzlau, P. Knaus, T. Holien, A. Bracher, C. Meyners, P. Czodrowski, V. Krewald, F. Hausch, *Chem. Sci.* **2021**, *12*, 14758.

[33] S. Pomplun, Y. Wang, A. Kirschner, C. Kozany, A. Bracher, F. Hausch, *Angew. Chem. Int. Ed.* **2015**, *54*, 345.

[34] A. M. Voll, C. Meyners, M. C. Taubert, T. Bajaj, T. Heymann, S. Merz, A. Charalampidou, J. Kolos, P. L. Purder, T. M. Geiger, P. Wessig, N. C. Gassen, A. Bracher, F. Hausch, *Angew. Chem. Int. Ed.* **2021**, *60*, 13257.

[35] Y. Wang, A. Kirschner, A.-K. Fabian, R. Gopalakrishnan, C. Kress, B. Hoogeland, U. Koch, C. Kozany, A. Bracher, F. Hausch, *J. Med. Chem.* **2013**, *56*, 3922.

[36] C. Kozany, A. März, C. Kress, F. Hausch, *ChemBioChem* **2009**, *10*, 1402.

[37] M. T. Gnatzy, T. M. Geiger, A. Kuehn, N. Gutfreund, M. Walz, J. M. Kolos, F. Hausch, *ChemBioChem* **2021**, *22*, 2257.

[38] "14:00-17:00. ISO 10993–5:2009. ISO.", can be found under http://www.iso.org/standard/36406.html (2022-12-11).

[39] A. Galat, *J. Chem. Inf. Model.* **2008**, *48*, 1118.

[40] J. R. Walker, M. P. Hall, C. A. Zimprich, M. B. Robers, S. J. Duellman, T. Machleidt, J. Rodriguez, W. Zhuo, *ACS Chem. Biol.* **2017**, 1028.

[41] E. P. Coutant, G. Gagnot, V. Hervin, R. Baatallah, S. Goyard, Y. Jacob, T. Rose, Y. L. Janin, *Chem. Eur. J.* **2020**, *26*, 948.

[42] R. I. Jepras, R. B. Fitzgeorge, A. Baskerville, *J. Hyg.* **1985**, *95*, 29.

[43] ISO 20776–2:2021 (en), "Clinical laboratory testing and in vitro diagnostic test systems – Suscepti-bility testing of infectious agents and evaluation of performance of antimi-crobial susceptibility test devices – Part 2: Evaluation of performance of antimicrobial susceptibility test devices against reference broth micro-dilution.", can be found under http://www.iso.org/obp/ui/#iso:std:iso:20776:-2:ed-2:v1:en (2022-12-11).